

Water retention properties of porous geopolymers for use in cooling applications

Kiyoshi Okada^{a,b,*}, Asami Ooyama^a, Toshihiro Isobe^a,
Yoshikazu Kameshima^a, Akira Nakajima^a, Kenneth J.D. MacKenzie^c

^a Department of Metallurgy and Ceramics Science, Tokyo Institute of Technology, 2-12-1 O-okayama, Meguro, Tokyo 152-8552, Japan

^b Materials and Structures Laboratory, Tokyo Institute of Technology, 4259 Nagatsuta, Midori, Yokohama, Kanagawa 226-8503, Japan

^c School of Chemical and Physical Sciences, Victoria University of Wellington, P.O. Box 600 Wellington, New Zealand

Received 20 September 2008; received in revised form 5 November 2008; accepted 6 November 2008

Available online 17 December 2008

Abstract

A series of geopolymers were prepared with varying ratios of sodium silicate, metakaolinite, NaOH and H₂O and their porous properties, water retention and mechanical properties were determined, to develop materials for counteracting heat island effects. Samples were prepared with the molar ratios SiO₂:Al₂O₃:Na₂O:H₂O of 3.66:1:x:y, where $x = 0.92\text{--}1.08$ and $y = 14.2\text{--}19.5$. The porous and mechanical properties of the geopolymers showed a good correlation with the H₂O/Al₂O₃ ratio (y); an increase in y produced an increase in the pore volume (from 0.26 to 0.46 ml/g), the pore size (from 15 to 390 nm) and the water absorption (from 27.2 to 51.1%). The same increase in y decreased the bulk density (from 1.29 to 0.99 g/cm³), the bending strength (from 14.2 to <5 MPa) and the water retention. Thus, the H₂O/Al₂O₃ ratio is the most important factor for controlling the porous properties of these materials, since geopolymers with higher H₂O/Al₂O₃ ratios are more porous and have higher water absorption rates, making them suitable as materials for surface cooling by water evaporation. Geopolymers with lower H₂O/Al₂O₃ ratios are more suitable for water retention applications, and have the advantage of higher mechanical strength.

© 2008 Elsevier Ltd. All rights reserved.

Keywords: Geopolymer; Porosity; Sol–gel processes; Silicate; Structural applications

1. Introduction

Rising temperatures in big cities are presenting an increasing problem, especially in the summer. This effect arises from the increasing amount of heat generated by human activity (vehicles, air conditioners, etc.) and because of the increasing surface areas covered by artificial materials with high solar absorption capacity. For example, the average temperature in Tokyo has increased 3–4 °C during the last 100 years. Related to this warming, the number of nights in which the temperature in Tokyo does not fall below 25 °C (known as “tropical nights”) has increased from 10–15 a decade or so ago to about 40 at present. This warming phenomenon is called the “heat island effect”. As one possible method for counteracting the heat island effect, we have investigated a passive cooling system using evaporation

of water absorbed by porous ceramics.^{1,2} Porous ceramics prepared from the clay minerals vermiculite and allophane¹ showed high water absorption, a fast absorption rate and a slow rate of water release rate due to their unique porous microstructure. By contrast, lotus-type porous ceramics prepared by extrusion using flammable fibers as the pore formers showed excellent capillary lift and water evaporation properties resulting from the controlled pore structure.²

Although the porous ceramics previously developed by our group show high water retention and good cooling effects due to their excellent capillary lift of water, it would be of considerable advantage if such porous ceramics could be prepared by a more environmentally friendly process without the need for firing at high temperatures. Geopolymers are good candidates for this purpose, since they are synthesized and hardened at ambient temperatures by the formation of a framework structure of alkali aluminosilicate gel. The term geopolymer was first proposed by Davidovits³ to describe inorganic aluminosilicate polymers formed from geological materials (clays), and

* Corresponding author. Tel.: +81 3 5734 2524; fax: +81 3 5734 3355.
E-mail address: okada.k.ab@m.titech.ac.jp (K. Okada).

many subsequent studies have been reported.^{4–8} The synthesis is generally performed by reacting an alkali silicate solution with a solid aluminosilicate such as metakaolinite, fly ash, etc., under alkaline conditions. The microstructure and mechanical properties are known to depend strongly on the chemical compositions of the starting materials. A review by Duxson et al.⁵ indicates a trend towards increased mechanical strength at higher $\text{SiO}_2/\text{Al}_2\text{O}_3$ ratios and increased porosity at higher $\text{H}_2\text{O}/\text{SiO}_2$ ratios. They also report that the microstructures of geopolymers change significantly at a $\text{SiO}_2/\text{Al}_2\text{O}_3$ ratio of about 3; below this ratio, geopolymers were more highly porous whereas above this ratio they were largely homogeneous.⁵ A maximum compressive strength of 70 MPa was observed at a $\text{SiO}_2/\text{Al}_2\text{O}_3$ ratio of 3.8.

In the present work, geopolymers were prepared by reaction of sodium silicate and metakaolinite in alkaline solution at temperatures close to ambient, using a range of $\text{Na}_2\text{O}/\text{Al}_2\text{O}_3$ and $\text{H}_2\text{O}/\text{Al}_2\text{O}_3$ ratios. The porous properties, water absorption and water release, and the mechanical properties of the resulting geopolymers were determined to assess their suitability as materials for counteracting heat island effects.

2. Experimental procedure

2.1. Preparation of the geopolymers

The starting materials were sodium silicate solution ($\text{Na}_2\text{O}/\text{SiO}_2 = 0.5$, Kanto Chemicals, Japan) and metakaolinite ($\text{Al}_2\text{Si}_2\text{O}_7$, prepared from Georgia kaolinite dehydroxylated at 600 °C for 24 h). These reagents were mixed with NaOH solution (Wako Chemicals, Japan) using a planetary homogenizer (ARE-250, THINKY, Japan) operated at 2000 rpm for 30 s. The molar ratios $\text{SiO}_2:\text{Al}_2\text{O}_3:\text{Na}_2\text{O}:\text{H}_2\text{O}$ were 3.66:1: x : where x varied from 0.92 to 1.08 and y varied from 14.2 to 19.5. Details of the nine resulting samples and their measured properties are listed in Table 1. The homogenized slurry was cast into an airtight container ($34 \times 34 \times 10 \text{ mm}^3$) which was half-filled with sample and cured at 40 °C for 4 days. The low curing temperature was chosen to avoid cracking.⁹ The geopolymer samples were then dried at 40 °C for 4 days.

2.2. Characterization

The bulk densities of the samples were determined by Archimedes' Principle and the pore size distribution and pore volume was measured by mercury intrusion porosimetry (Auto Pore IV 9520, Shimadzu, Japan) at a maximum injection pressure of 200 MPa. The contact angle and surface tension used for the calculation was 130° and 0.485 N/m, respectively. The measurements up to such a high injection pressure may cause collapsing of pore structure of the samples during the Hg porosimetry. If collapsing occurs during the measurements, the pore size distribution curves should show some anomaly. No anomaly was, however, observed in the curves and also the samples kept the original shape after the experiments, indicating effectiveness of the measurements. X-ray measurements

Table 1
Various data of geopolymer samples.

Sample	NaOH [M]	$\text{Na}_2\text{O}/\text{Al}_2\text{O}_3$	$\text{H}_2\text{O}/\text{Al}_2\text{O}_3$	Bulk density [g/cm^3]	Pore volume [ml/g]	Pore size [nm]	Bending strength [MPa]	Water absorption [%]	FWA [%/min]	JWR [%/day]
S15	6	1.08	15.4	1.18	0.35	53	–	31.2	29.6	4.2
S17	6	1.08	17.4	1.11	0.41	130	–	41.1	39.0	5.7
S19	6	1.08	19.5	0.99	0.46	390	<5	51.1	47.2	9.1
N15	10	1.00	14.6	1.22	0.32	30	–	28.8	19.1	3.6
N17	10	1.00	16.6	1.15	0.39	54	9.8(13) [#]	36.4	31.1	4.0
N19	10	1.00	18.6	1.07	0.44	110	–	43.5	41.9	6.7
R15	14	0.92	14.2	1.29	0.26	15	14.2(14)	27.2	14.0	0.8
R17	14	0.92	16.3	1.19	0.33	26	–	32.0	23.3	4.0
R19	14	0.92	18.2	1.08	0.39	43	–	38.7	35.4	4.5

[#] The numbers in the parentheses is standard deviation at the last decimal place.

were performed using monochromated Cu K α radiation (XRD-6100, Shimadzu, Japan) to identify the phases formed. The DTA/TG curves were recorded up to 1000 °C at a heating rate of 10 °C/min using a sample weight of about 15 mg (Thermoplus TG8120, Rigaku, Japan). Solid-state ^{29}Si and ^{27}Al MAS NMR spectra were obtained at 11.7 T using a Varian Unity 500 spectrometer and Doty MAS probe spun at 10–12 kHz. The ^{29}Si spectra were acquired using a 90° pulse of 60 μs and a recycle delay time of 100 s, and were referenced to tetramethylsilane (TMS). The ^{27}Al spectra were acquired using a 15° pulse of 1 μs and a recycle delay time of 1 s and were referenced to $\text{Al}(\text{H}_2\text{O})_6^{3+}$. The microstructures of the samples after sputtering with Pt were observed using a SEM (JSM-5310, JEOL, Japan) at an accelerating voltage of 20 kV. The four-point bending strengths of the samples were measured on unpolished test pieces ($5 \times 4 \times 30 \text{ mm}^3$) using a universal testing machine (Autograph DCS-R-10TS, Shimadzu, Japan) at a cross-head speed of 0.5 mm/min. The average bending strength was obtained from measurements of 10 samples.

2.3. Water retention properties

Water retention property measurements were carried out by placing the samples in a desiccator in which the relative humidity (RH) was controlled at 53% (25 °C) by the presence of saturated $\text{Mg}(\text{NO}_3)_2 \cdot 6\text{H}_2\text{O}$ solution. Samples thus equilibrated for 24 h are designated humidity-saturated samples (W_0). The water absorption of the W_0 samples was determined by immersing them in deionized water at 25 °C and weighing after pre-determined time intervals up to 24 h. The water absorbed after 24 h was defined as the water absorption (WA (%)). The initial water absorption rate (IWA (%/min)) was calculated from the slope of the water absorption curves. Release of the absorbed water was measured by returning the sample to the desiccator at $\text{RH} = 53\%$ and re-weighing at intervals up to 12 days. The initial water release rate (IWR (%/day)) was calculated from the slope of the water release curves.

3. Results and discussion

3.1. Geopolymers

The geopolymer products set and hardened without apparent shrinkage, forming pale yellow-brown slabs with smooth surfaces. The XRD patterns of all the samples showed a halo at 25–30° 2 θ corresponding to typical X-ray amorphous gel structures. The measured bulk densities of the samples, shown in Fig. 1 as a function of the $\text{H}_2\text{O}/\text{Al}_2\text{O}_3$ ratio, range from 0.99 to 1.29 g/cm 3 and clearly show a trend of decreasing bulk density with increasing $\text{H}_2\text{O}/\text{Al}_2\text{O}_3$ ratio. This suggests that excess H_2O in the synthesis is not included in the framework structure of the geopolymers and causes the bulk density of the porous matrix to decrease. The pore size distributions (PSDs) of samples S19, N17 and R15 (Fig. 2) show a sharp increase in the cumulative pore volume curve at pore sizes of 15 nm, 54 nm and 390 nm in samples R15, N17 and S19 respectively. These pore sizes correspond to an increase in the total pore volumes of 0.26–0.46 ml/g

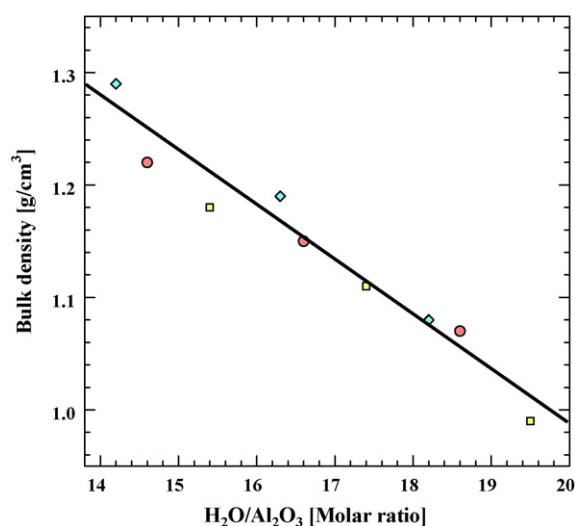


Fig. 1. Bulk density of the geopolymer samples as a function of their $\text{H}_2\text{O}/\text{Al}_2\text{O}_3$ ratio.

with increasing $\text{H}_2\text{O}/\text{Al}_2\text{O}_3$ ratios in these three samples. Thus, although the microstructures of these samples may be similar, their pore sizes differ. The pore volumes and pore sizes of all nine samples are shown in Fig. 3 as a function of their $\text{H}_2\text{O}/\text{Al}_2\text{O}_3$ ratio. The pore volumes increase with increasing $\text{H}_2\text{O}/\text{Al}_2\text{O}_3$ ratio, but are also slightly influenced by the $\text{Na}_2\text{O}/\text{Al}_2\text{O}_3$ ratio, as evidenced by the three samples where $\text{Na}_2\text{O}/\text{Al}_2\text{O}_3 = 1.08$, which show lower pore volumes than the other series of samples. The effect of the $\text{Na}_2\text{O}/\text{Al}_2\text{O}_3$ ratio is seen more clearly in the pore size results; although the three series of samples with different $\text{Na}_2\text{O}/\text{Al}_2\text{O}_3$ ratios show increased pore size with increasing $\text{H}_2\text{O}/\text{Al}_2\text{O}_3$ ratio, the plots of these parameters (Fig. 3) are different for the three series. The pore sizes increase with decreasing $\text{Na}_2\text{O}/\text{Al}_2\text{O}_3$ ratio in samples with the same $\text{H}_2\text{O}/\text{Al}_2\text{O}_3$ ratio. Thus, the porous properties of these geopolymers can be varied significantly by changing both the $\text{H}_2\text{O}/\text{Al}_2\text{O}_3$ ratio (the major

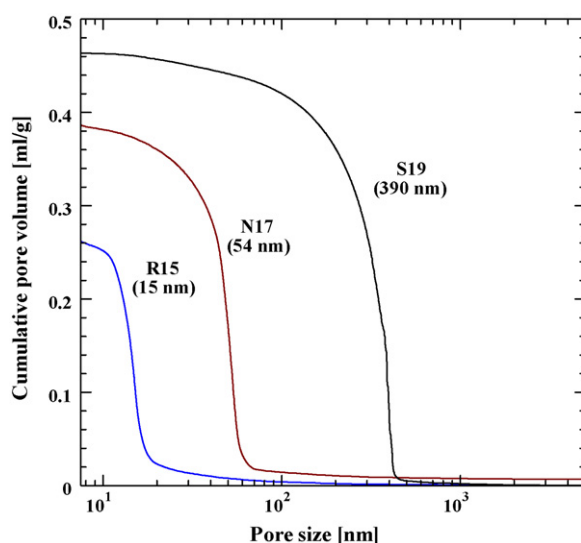


Fig. 2. Cumulative pore volume curves of samples S19, N17 and R15.

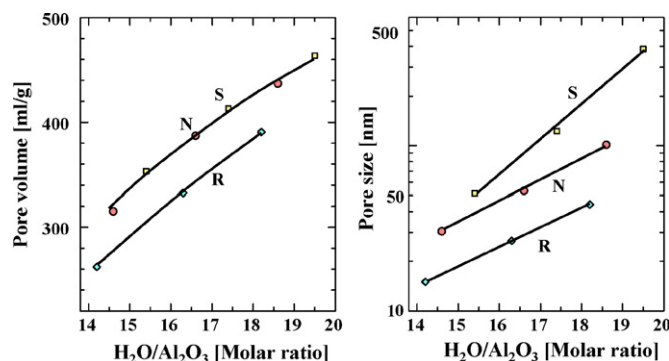


Fig. 3. Pore volumes and pore sizes of the samples as a function of their $\text{H}_2\text{O}/\text{Al}_2\text{O}_3$ ratio.

effect) and the $\text{Na}_2\text{O}/\text{Al}_2\text{O}_3$ ratio (the minor effect). Since we prepared those samples by changing the concentration of NaOH solution but fixing the dosages of water glass and metakaolinite, the effect of NaOH concentrations is also taken into consideration.

Since the geopolymer samples were X-ray amorphous, they were examined by ^{29}Si and ^{27}Al MAS NMR. The spectra of sample N17 are shown in Fig. 4. The ^{27}Al MAS NMR spectrum shows a predominant sharp resonance at about 59 ppm, with a trace of a minor peak at 4 ppm. Very similar ^{27}Al spectra were also recorded for all the other samples. The resonance at 59 ppm corresponds to Al in 4fold coordination,¹⁰ confirming the presence of the AlO_4 tetrahedra that compose the three-dimensional tetrahedral framework structure of geopolymer gels. The distinct resonance at -90 ppm in the ^{29}Si MAS NMR spectrum (Fig. 4) was also found in all the other samples. This resonance is at a similar position but of narrower line width to the spectrum reported for a geopolymer with $\text{Si}/\text{Al}=1.65$.⁶ This broad ^{29}Si peak could contain four possible overlapping resonances corresponding to $\text{Si Q}^4(m\text{Al})$ species, where $m=1-4$). The narrow peak widths of the present samples suggest that the main $\text{Si Q}^4(m\text{Al})$ species may be $m=2$ and 3. The similarity of the ^{29}Si and ^{27}Al MAS NMR spectra of all nine samples indicates that their structures are very similar, consistent with their identical

$\text{SiO}_2/\text{Al}_2\text{O}_3$ ratio, and further, varying the $\text{Na}_2\text{O}/\text{Al}_2\text{O}_3$ ratio has a negligible effect on the structure.

The microstructures of the three samples S19 (the most porous), N17 (of intermediate porosity) and R15 (the most dense) are shown in Fig. 5a–c, respectively. The microstructures of N17 and R15 are similar, consisting of a homogeneous matrix with dispersed platy particles (residual metakaolinite). Although the content of platy particles in these samples seems from the micrographs to be considerable, there is no indication of the 5fold coordinated ^{27}Al MAS NMR resonance at about 30 ppm arising from metakaolinite. By contrast, the microstructure of sample S19 consists of agglomerated fine particles and less platy particles than in the other two samples. The difference in the microstructure of sample S19 by comparison with the two other samples may arise from the different amounts of H_2O and NaOH used in their syntheses.

The mechanical strength of sample S19 was too weak to be measured (<5 MPa), but the strengths of samples N17 and R15 were found to be 9.8(13) MPa and 14.2(14) MPa respectively. The numbers in the parentheses represent the standard deviation in the last decimal places. These strengths are similar to those reported by Luz Granizo et al.¹¹ The trends in the strengths of the present geopolymers are consistent with the other properties of these samples (Table 1). The relatively low strengths suggest the presence of large flaws and the possibility that defects are introduced during the moulding of the precursor slurry. Bubbles are likely to be included in the slurry during homogenization and their removal may require vacuum outgassing rather than simply tapping or vibrating the mould. The enhancement of mechanical strength may be needed for some applications.

3.2. Water retention properties

The relationship between the water absorption (WA) and the $\text{H}_2\text{O}/\text{Al}_2\text{O}_3$ ratio of the samples (Fig. 6) clearly shows an increase in WA with increasing $\text{H}_2\text{O}/\text{Al}_2\text{O}_3$ ratios. Sample R15 shows the lowest value of WA (27.2%) and sample S19 the highest (51.1%). As explained above, the WA values are calculated from the amount of water absorbed from the sample saturated

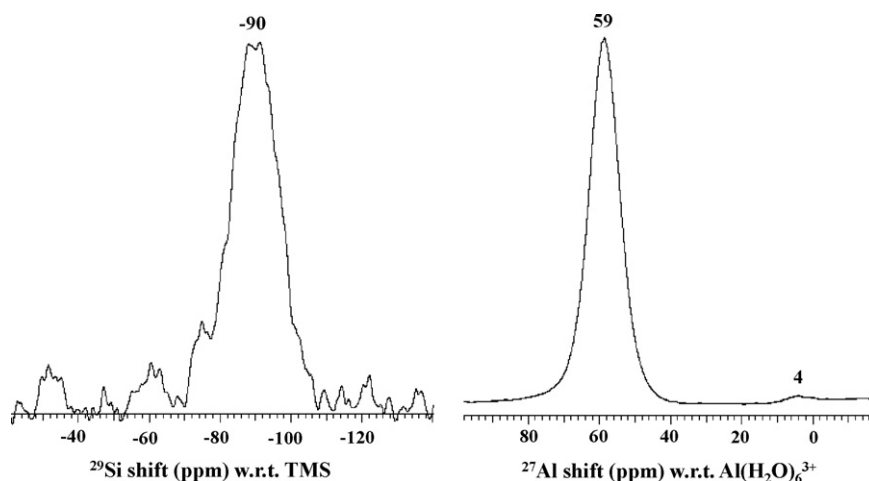


Fig. 4. 11.7T ^{29}Si and ^{27}Al MAS NMR spectra of sample N17.

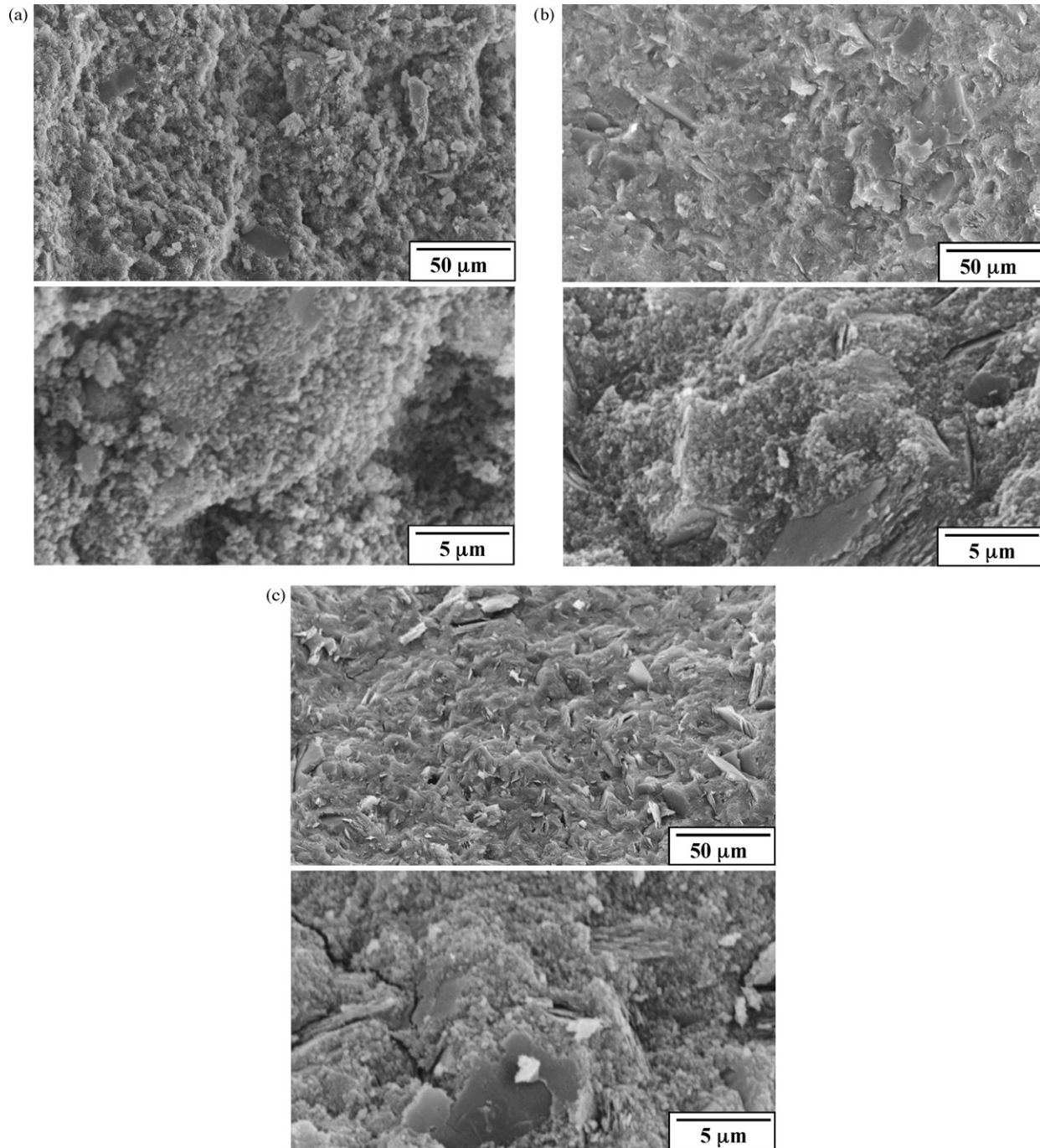


Fig. 5. SEM micrographs of fractured surfaces of samples S19 (a), N17 (b) and R15 (c).

at $RH = 53\%$ (W_0) and not from the fully dry sample. Thus, the actual amounts of water in the samples are greater than the WA values. The water content of the W_0 samples was measured by TG, which showed in all cases a steep weight loss at 200°C followed by a more gradual loss up to about 600°C . The total weight loss was very similar in all samples, ranging from 19% in sample R15 to 21% in sample S19.

After the measurement of WA , the samples were placed in the desiccator at $RH = 53\%$ and their water release property determined from their weight change. This release of absorbed water, shown in Fig. 7 as a function of release time, occurs almost lin-

early with time except in the case of sample R15, and is almost complete in all the samples after 6–9 days. The release rates vary from sample to sample, being faster in the samples of higher WA . The water release curve of sample R15 is quite different in shape from those of the other samples, possibly related to the very small pore size of this sample. Since the water absorption and release rates in these samples should correspond to their pore sizes, both the IWA and IWR data are plotted in Fig. 8 as a function of the sample pore size. As expected, both the IWA and IWR values show good relationships with pore size, since the samples with larger pore sizes have higher IWA and IWR values.

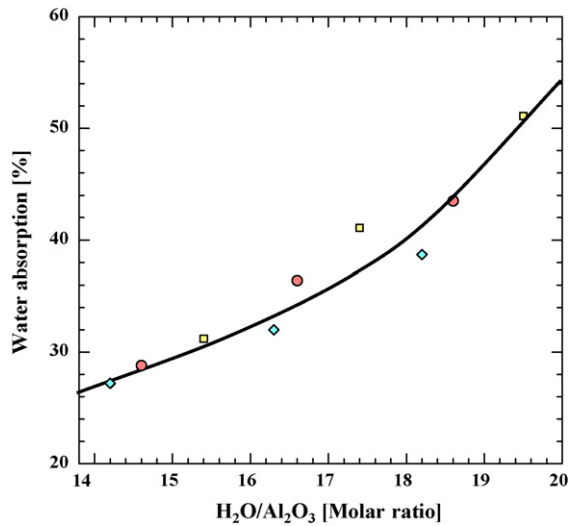


Fig. 6. Water absorption of the samples as a function of their $\text{H}_2\text{O}/\text{Al}_2\text{O}_3$ ratio.

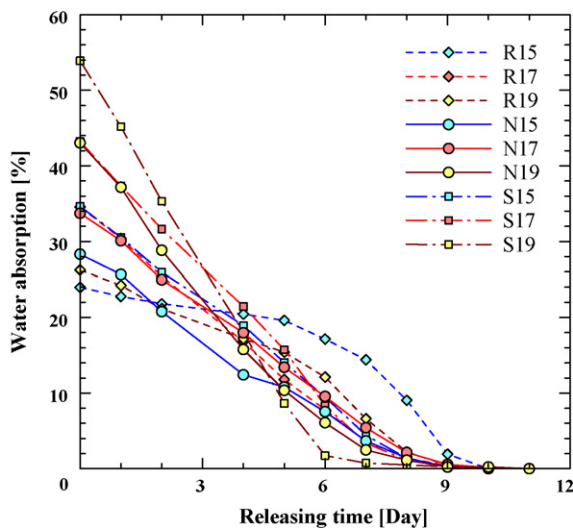


Fig. 7. Water absorption values of the samples as a function of the release time in a 53% RH atmosphere.

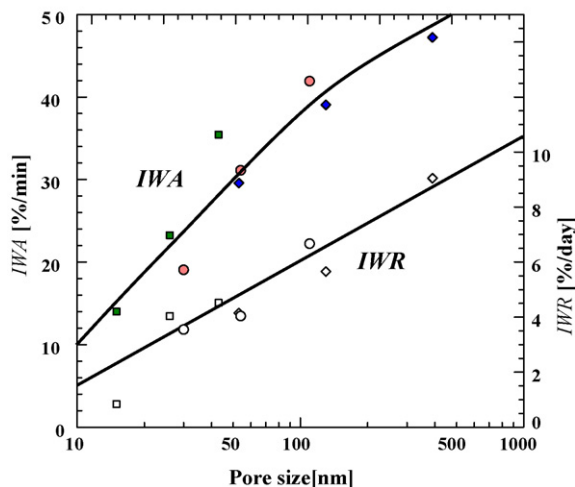


Fig. 8. IWA and IWR values of the samples as a function of their $\text{H}_2\text{O}/\text{Al}_2\text{O}_3$ ratio.

In this study, the chemical compositions of the geopolymers (in terms of their $\text{H}_2\text{O}/\text{Al}_2\text{O}_3$ and $\text{Na}_2\text{O}/\text{Al}_2\text{O}_3$ ratios) were systematically varied, allowing the porosity and water retention properties to be adjusted over a relatively wide range of values, especially by altering the $\text{H}_2\text{O}/\text{Al}_2\text{O}_3$ ratio. Geopolymers synthesized with higher $\text{H}_2\text{O}/\text{Al}_2\text{O}_3$ ratios are more porous, their larger pore size and higher pore volume giving them good water absorption and water retention properties but decreasing their mechanical strength. The limited mechanical strength of this type of geopolymers may have restriction on some applications. By contrast, the geopolymers synthesized with lower $\text{H}_2\text{O}/\text{Al}_2\text{O}_3$ ratios are denser, with smaller pore sizes and lower pore volumes, resulting in better water retention and mechanical properties than materials with higher $\text{H}_2\text{O}/\text{Al}_2\text{O}_3$ ratios. Thus, the two types of geopolymers are suitable for different water retention applications. The water absorption and capillary lift properties of geopolymers synthesized with higher $\text{H}_2\text{O}/\text{Al}_2\text{O}_3$ ratios could be enhanced by the introduction of pores generated by thermal and/or chemical treatment of organic pore-forming fibers.

4. Conclusion

Nine compositions of aluminosilicate geopolymers were prepared with differing $\text{H}_2\text{O}/\text{Al}_2\text{O}_3$ and $\text{Na}_2\text{O}/\text{Al}_2\text{O}_3$ ratios and their porous and mechanical properties and water retention was investigated. The following results were obtained:

- (1) The $\text{H}_2\text{O}/\text{Al}_2\text{O}_3$ ratio exerts a major effect on the physical properties; higher ratios result in increased pore volumes and pore sizes, and therefore thus higher water absorption ability, whereas lower $\text{H}_2\text{O}/\text{Al}_2\text{O}_3$ ratios increase the bulk density and mechanical strength.
- (2) At the lowest $\text{H}_2\text{O}/\text{Al}_2\text{O}_3$ ratio used here (14.2), the highest mechanical strength (about 14 MPa) was recorded.
- (3) The water retention properties of the samples depend on their pore size, larger sizes giving both higher water absorption and water release rates. Thus, the slow water release properties required in materials for remediation of heat island effects will be better satisfied by geopolymers with lower $\text{H}_2\text{O}/\text{Al}_2\text{O}_3$ ratios.

Acknowledgements

We are grateful to Professor Y. Matsuo of Tokyo Institute of Technology for permitting the use of the mechanical testing machine and Professor M. Daimon, for the Hg porosimeter.

References

1. Okada, K., Matsui, S., Isobe, T., Kameshima, Y. and Nakajima, A., Water-retention properties of porous ceramics prepared from mixtures of allophane and vermiculite for materials to counteract heat island effects. *Ceram. Intern.*, 2008, **34**, 345–350.
2. Okada, K., Kameshima, Y., Nakajima, A. and Madhusoodana, C. D., Preparation of lotus-type porous ceramics with high water pump-up ability and its cooling effect by water evaporation. *J. Heat Island Inst. Intern.*, 2007, **2**, 1–5.

3. Davidovits, J., Inorganic polymeric new materials. *J. Therm. Anal. Calor.*, 1991, **37**, 1633–1656.
4. Barbosa, V. F. F. and MacKenzie, K. J. D., Synthesis and thermal behaviour of potassium sialate geopolymers. *Mater. Lett.*, 2003, **57**, 1477–1482.
5. Duxson, P., Provis, J. L., Lukey, G. C., Mallicoat, S. W., Kriven, W. M. and Deventer, J. S. J., Understanding the relationship between geopolymer composition, microstructure and mechanical properties. *Colloids Surf.*, 2005, **269**, 47–58.
6. Duxson, P., Fernandez-Jimenez, A., Provis, J. L., Lukey, G. C., Palomo, A. and vanDeventer, J. S. J., Geopolymer technology: the current state of the art. *J. Mater. Sci.*, 2007, **42**, 2917–2933.
7. Panagiotopoulou, Ch., Kontori, E., Perraki, Th. and Kakali, G., Dissolution of aluminosilicate minerals and by-products in alkaline media. *J. Mater. Sci.*, 2007, **42**, 2967–2973.
8. van Deventer, J. S. J., Provis, J. L., Duxson, P. and Lukey, G. C., Reaction mechanisms in the geopolymeric conversion of inorganic waste to useful products. *J. Hazard. Mater.*, 2007, **A139**, 506–513.
9. Perera, D. S., Uchida, O., Vance, E. R. and Finnie, K. S., Influence of curing schedule on the integrity of geopolymers. *J. Mater. Sci.*, 2007, **42**, 3099–3106.
10. MacKenzie, K. J. D. and Smith, M. E., Multinuclear Solid-State NMR of Inorganic Materials. *Pergamon Materials Series, vol. 6*. Pergamon, Oxford, 2002.
11. Luz Granizo, M., Blanco-Varela, M. T. and Martinez-Ramirez, S., Alkali activation of metakaolinites: parameters affecting mechanical, structural and microstructural properties. *J. Mater. Sci.*, 2007, **42**, 2934–2943.